



## PROPERTIES OF GE-DOPED SILICA PREFORM BY RAMAN SPECTROSCOPY

A. S Siti Shafiqah<sup>1,2</sup>, Y. M Amin<sup>1</sup>, R. Md Nor<sup>1</sup>, N. Tamchek<sup>2</sup>, Khairul Anuar M. S<sup>3</sup>, H. A Abdul Rashid<sup>4</sup> and D. A Bradley<sup>5</sup>

<sup>1</sup>Department of Physics, Faculty of Science, Universiti Malaya, Kuala Lumpur, Malaysia

<sup>1</sup>Department of Physics, Kuliyyah of Science, International Islamic University Malaysia

<sup>2</sup>Department of Physics, Fac. of Science, Universiti Putra Malaysia, Selangor, Malaysia

<sup>3</sup>Advance Physical Technologies, Telekom Research and Development Cyberjaya, Malaysia

<sup>4</sup>Faculty of Engineering, Multimedia University, Cyberjaya, Malaysia

<sup>5</sup>Department of Physics, University of Surrey, Guildford, UK

E-Mail: [shafiqahshaharuddin22@gmail.com](mailto:shafiqahshaharuddin22@gmail.com)

### ABSTRACT

In the present work, the structural modifications of Ge-doped silica preforms due to  $\gamma$ -irradiation at room temperature have been investigated using Raman spectroscopy. The MCVD fabricated preforms labelled as P1 and P2 are distinguishable by the oxidation and thermal history during the fabrication process, in which related to the oxygen bonding of SiO<sub>4</sub> tetrahedral. From Raman analysis, the 480 cm<sup>-1</sup>(D1) and 609 cm<sup>-1</sup>(D2) peaks are the main network features of pure and doped silica glass, suggest the formation of defect centers in the preforms. The structural modifications of this defects centers are more sensitive in P2, due to the oxygen deficient state of the preform.

**Keywords:** Ge doped silica perform, raman spectroscopy- MCVD, oxygen-deficient.

### INTRODUCTION

Recent study shows that under certain circumstances of fabrication parameter (i.e. pressure, precursor flow, temperature and collapse speed), specific defect condition can occur (Lü *et al.* 2014; Salh, 2011; Shen *et al.* 2013). The condition for defect to form is mainly determined by the oxidation (annealing) environment during the process which later can be classified into oxygen rich or oxygen deficient center (ODC) (Ballato and Dragic, 2013; Pasquarello and Car, 1998). The ODC is responsible for many photo-induced transformations that is significant to the development of electronic and optical devices (Salh, 2011; Skuja, 1998). The understanding in the effect of ODC in glass is limited, due to the nature of this defect as it is diamagnetic and hindered by electron-phonon interaction (Skuja, 1998). When the ODC is bleached by photon, this center transforms from diamagnetic into paramagnetic. This rearrangement of electron together with the atomic relaxation, results in the increasing of polarizability. For further investigation, we exposed our sample to gamma- irradiation in order to induce microstructure damage allowing the Si-O-Si coordination to be identified and studied. The structural modification of Ge-doped silica preform have been investigate using Raman spectroscopy.

Structural modification such as symmetric stretching and breathing motion in ring have been reported to be Raman scattering active (Pasquarello and Car, 1998; Salh, 2011; Shen *et al.* 2013). The number of Si-O-Si rings and their correspondants to the distribution under  $\gamma$  irradiation will be quantitatively investigate to understand the effect of preform quality on two different fabrication process.

### EXPERIMENTATION

#### Preformed fabrication via MCVD

The preforms have been fabricated using modified chemical vapor deposition (MCVD) technique labelled as P1 and P2. The MCVD process utilized vapor mixture of highly purity Silica Tetrachloride (SiCl<sub>4</sub>) and Germanium Tetrachloride (GeCl<sub>4</sub>) as starting material (Nagel *et al.* 1982; Wood *et al.* 1987)]. The mixture are oxidised by O<sub>2</sub> gas being heated with external high temperature oxy-hydrogen flame to form a fine glass particle 'soot'. The vapor mixture flowed into a silica glass tube which also serve as a substrate. The 'soot' are then deposited on the inside walls of the glass tube at downstream of the flame moving direction due to the thermophoresis phenomena (Simpkins *et al.* 1979). The soot is immediately sintered to transparent, bubble-free high quality glass layer as the flame traverses over that soot position. By repeating the traversal process again, the build-up of the glass layer is done. When the required glass thickness is attained, the tube substrate is heated closed to silica glass fictive temperature (1900 – 2100 °C) which reduced the tube diameter slowly (collapse process) and finally produced a solid glass rod known as preform. During collapse process, O<sub>2</sub> flowed into the substrate tube to preserve its inner pressure and to avoid volatilization of GeO<sub>2</sub> from the core. The O<sub>2</sub> flow rate are gradually reduced as the tube diameter decreased and finally stop when the tube inner diameter started to fuse.

This MCVD technique are widely exploit in optical fiber fabrication due to the highly pure starting precursor with low impurities (i.e. transition metal ions and OH-ions) glass for long distance optical communication network (Bubnov *et al.* 2004; MacChesney, 2000). The final quality of the optical glass



such as optical loss/attenuation, refractive index and shape can be controlled by varying the precursor flow and process temperature (i.e. oxidation and annealing) (Ainslie *et al.* 1982).

In the present work, two types of sample are employed with the precursor flow rate and deposition temperatures are shown in Table-1. The collapsing rate is defined as the speed of the hydrogen-oxygen torch moving from end to end of the preform and the collapse temperature is fixed similar to oxidation temperature. Due to high temperature, substrate tube experienced stronger distortion and also greater GeO<sub>2</sub> volatilization rate (Bubnov *et al.* 2004; MacChesney, 2000; Nagel *et al.* 1982; Simpkins *et al.* 1979; Wood *et al.* 1987). The final solid glass rod is cut to small glass disk (thickness about 2.0 ± 0.2 mm) and polished for optical quality using diamond sand paper. The GeO<sub>2</sub> concentration, distribution and also refractive index (RI) were determined using x-ray energy dispersion technique (FEG Quanta 450, EDX Oxford) and preform profiler (Photon Kinetic PK 104).

**Table-1.** Precursor flow rate and deposition temperature.

Precursor/Process	Sample P1	Sample P2
SiCl <sub>4</sub> vapor flow	100	100
GeCl <sub>4</sub> vapor flow	200	150
O <sub>2</sub> flow	1400	1600
Oxidation temperature (°C)	2100	2200
Collapsing rate [mm/min] (torch speed)	2	4

#### a) Raman spectroscopy

Raman scattering measurements were carried out for all preforms by using Renishaw inVia Raman spectrometer in room temperature. The excitation laser was focused to the sample with 50x objective lens from 532 nm (DPSS) laser with power of 25mW. The scattering intensity light collected at 90° to the excitation beam are dispersed with 1800lines/mm dispersive grating through a 65 μm pin-hole then detected using peltier-cooled CCD. The spectral resolution of the dispersive spectrometer is 1.1 cm<sup>-1</sup>. All the Raman intensity have been corrected for temperature dependence, as shown in equation (1), using Bose-Einstein equation (2) [27],

$$I_{corrected} = \frac{I_{observed}}{n(\omega) + 1} \quad (1)$$

$$n(\omega) = \exp\left(\frac{h\omega}{k_B T}\right) \quad (2)$$

$I_{corrected}$  = measured intensity in Raman spectra

$h$  = Plank's constant

$\omega$  = wavenumber in Raman spectra

$T$  = measurement temperature in Kelvin

$k_B$  = Boltzman's constant

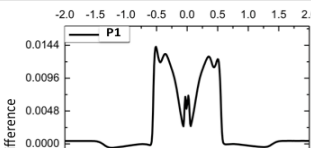
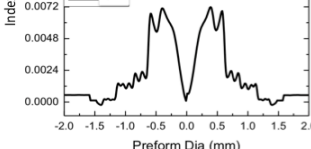
The Raman spectra are then normalized to the Si-O-Si symmetric stretching of bridging oxygen (BO) dominant band around 440 cm<sup>-1</sup> where this band are predominant for 6-membered SiO<sub>4</sub> (Vaccaro *et al.* 2010).

## RESULTS AND DISCUSSION

#### Fiber analysis

The refractive index profile (RIP) are then measured by using a preform profiler (Photon Kinetic PK104) to see the Ge mol% concentration in the preforms. Note from Table-1, the germanium has been proved to have the ability to increase the RIP of the silica. The cladding part of the preform consist only silica, while the core consist both of silica and germanium. The index difference between the core and the outer layer are about 1.44% (P1), and 0.72% (P2). The high index difference in the core shows that the germanium is highly doped in the core during the fabrication process.

**Table-2.** Refractive index profile (RIP) for sample P1 and P2.

Refractive index profile	Ge mol% (1.31x10 <sup>-3</sup> mol per index diff)	Core size(mm)
	8.54	1.40
	5.0	2.40

Analysis on the fiber have been carried out using x-ray energy dispersion analysis (EDX) to see the distribution of all elements in the preforms.

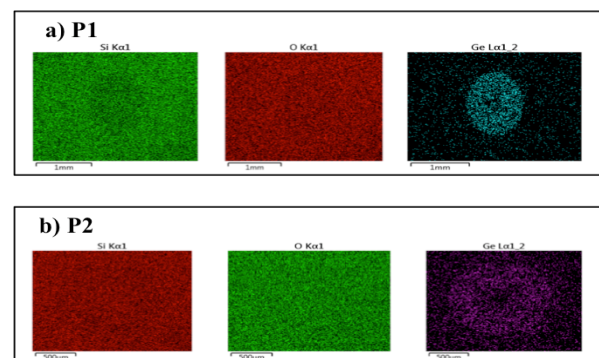


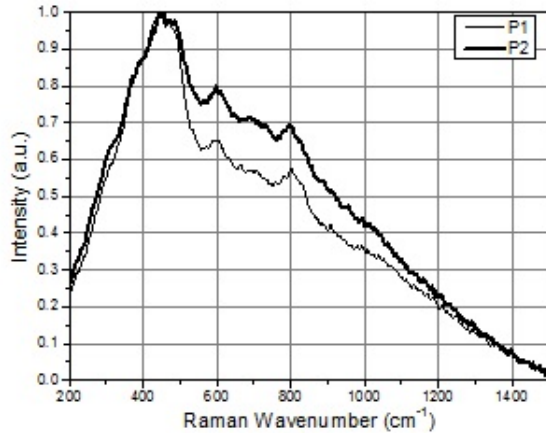
**Figure-2.** The distribution of silica, oxygen and germanium in P1 and P2.

By using mapping technique, Figure-1 shows the homogenous distribution of Silica, Oxygen and Germanium element in the core and cladding part for both

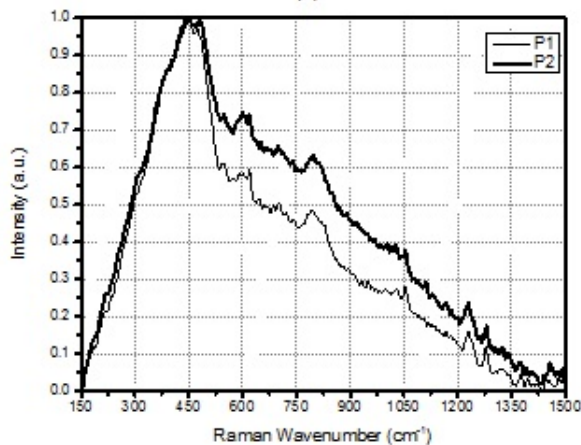


preform. This result agree with the RIP profile (Table-2), showing Ge is highly distributed in the core.

### a) Raman Spectroscopy



(a)



(b)

**Figure-2.** Raman spectra for both preforms a) before radiation b) after  $\gamma$ - irradiation with 10Gy. Note that the upper line (red) refers to P2 while the down line (blue) is P1. Main peak reveals at 440, 609, 800, 1060, 1230 and 1280  $\text{cm}^{-1}$ .

The Raman spectra of both sample before and after radiated with  $\gamma$  irradiation of 10 Gy is given in Figure-2 (a) and (b). Before radiation, both sample produces similar Raman peak wavenumber at  $\sim 440$ ,  $\sim 480$ , 600 and 800  $\text{cm}^{-1}$ . It has been reported that the broad region around 400-500  $\text{cm}^{-1}$  consist two main peaks situated at 440  $\text{cm}^{-1}$  and 480  $\text{cm}^{-1}$  (D1) [(Galeener, 1979; Vaccaro *et al.* 2010)]. Peak at 440  $\text{cm}^{-1}$  peak represents the symmetric stretching of bridging oxygen atoms with silicon (Si-O-Si)<sub>n</sub> with ring number of n=6 (Baur, 1980; Pasquarello and Car, 1998). The 480  $\text{cm}^{-1}$  (D1) is a defect mode, assigned to breathing motion of bridging oxygen in 4-membered SiO<sub>4</sub> rings (Baur, 1980).

From peak deconvolutions at this region, the Raman peaks were observed at 451 and 485  $\text{cm}^{-1}$  with the half width between 93 to 106  $\text{cm}^{-1}$ . The Raman shift have

been shifted to higher wavenumber around  $\sim 12$  cm from peak at 440  $\text{cm}^{-1}$  and it is dominated by the changes of bond length (compared with bond angle) which can be refer to the existence of tensile strain between Si-O bond and also phonon confinement effects (Galeener, 1979; Revesz and Walrafen, 1983; Sato and Suda, 1998). Peak at this region also represent strong, narrow and polarized GeO<sub>2</sub> raman scattering at 440 and 456  $\text{cm}^{-1}$  which is capable to shift the peak center wavenumber (Gillet *et al.* 1990; Sato and Suda, 1998). The dispersion of the peak half width about  $\sim 13$   $\text{cm}^{-1}$  from usual (Si-O-Si) symmetric stretching mode of bridging oxygen is also related to the incorporation of Ge atoms into Si-O-Si network (Gillet *et al.* 1990; Martinez *et al.* 2003).

As reported in (Revesz and Walrafen, 1983), peak at 480  $\text{cm}^{-1}$  (D1) is immune to particle irradiation thus no/small significant observation was found. The peak at 609  $\text{cm}^{-1}$  (D2) is clearly observed on both sample arise from symmetric stretching vibration of oxygen in a planar three membered (Si-O) 3 ring structures (Baur, 1980; Pasquarello and Car, 1998; Shen *et al.* 2013). The intensity of this band was found higher for sample P2 compared to P1 suggesting an enhancement of the (Si-O-Si)<sub>3</sub> ring structure. The enhancement is suspected from high mobility of Ge atoms during high temperature oxidation process that broke long-range SiO<sub>4</sub> tetrahedral structure. Later, when the sample cooled down to room temperature, the Ge atoms bond and forming a short bond with O atoms thus left down the (Si-O)<sub>3</sub> ring structure. From structural relaxation study shows this phenomenon might increase the material fictive density and the symmetric cooperative vibration (Jr. and Galeener, 1980).

As the effect of  $\gamma$ -radiation, the glass atomic structure is deformed and producing a point defect (Friebele *et al.* 1979). From quantitative studies of the Raman peak, the defect can be identified and their respective phonon interaction, bonding characteristics and strain can be analyzed. Note from Figure-1. (b), after irradiation, more Raman modes appear at 700, 800 1060, and 1230  $\text{cm}^{-1}$  region. The increasing number of these modes can be related to the deformation of Si-O-Si, Ge-Si, Ge-O and Si-Si bond (Gillet *et al.* 1990; Martinez *et al.* 2003; Sato and Suda, 1998). At region 600  $\text{cm}^{-1}$ , the peak is splitting and broaden slightly to higher wavenumber with decreasing intensity due to Ge-O-Ge bending modes. The weak band at 1060 and 1230  $\text{cm}^{-1}$  which are only apparent in the irradiate sample is assigned to Si-O-Si transverse-optical (TO) and longitudinal-optical (LO) symmetric-stretching and asymmetric stretching respectively with one, two, three and four non-bridging oxygen (Galeener, 1979, 1982; McMillan *et al.* 1994). While peak at 1230  $\text{cm}^{-1}$  shows the breakage of SiO<sub>2</sub> to metasilicate, Si<sub>2</sub>O<sub>6</sub> (Chmel and Sochivkin, 1986; McMillan, 1980).

Figure-3 is the absorption spectra reported by Shafiqah *et al* on the same sample used in this study. The result shows only in P2 sample, peak at 5.1 eV which assigned to the germanium oxygen-deficient sample (GODC) can be clearly observed. This result indicate that



the P2 is an oxygen deficient state while P1 is in an oxygen rich sample. Our results from Raman spectroscopy reveals the oxygen deficient samples are more sensitive to the structural modification by  $\gamma$ -irradiation, showing larger Raman intensity compared to the oxygen rich.

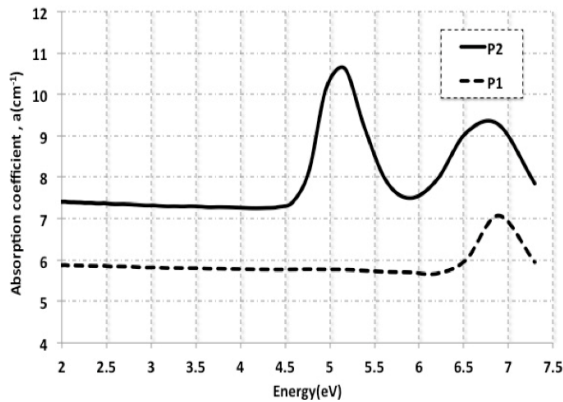


**Figure-3.** Absorption spectra for P1 and P2, with peak at 5.1 eV is assigned to the GODC only apparent in P2 (Shafiqah *et al.* 2015).

## CONCLUSIONS

In summary, we have examined the Raman scattering of Ge-doped SiO<sub>2</sub> optical preform fabricated by MCVD technique. Two types of sample were fabricated to study the influence of oxidation process parameter by adjusting the precursor concentration and process temperature. Although their final concentration is almost similar, oxygen-deficient sample is more sensitive to structural modification by  $\gamma$ -irradiation thus produces significant Raman scattering.

## ACKNOWLEDGEMENTS

The project is supported by High Impact Research Grant H-21001-F0033 and Postgraduate Research Fund PG065-2013A. We would like to thank members of the Low Dimensional Materials Research Center, University of Malaya and of the MCVD Laboratory, Multimedia University for their support.

## REFERENCES

- [1] Ainslie B.J., Beales K.J., Cooper D.M., Day C.R. and Rush J.D. 1982. Drawing-dependent transmission loss in germania-doped silica optical fibres. *J. Non. Cryst. Solids*, Vol. 47, pp. 243–245.
- [2] Ballato J. and Dragic P. 2013. Rethinking Optical Fiber: New Demands, Old Glasses. *J. Am. Ceram. Soc.* Vol. 96, pp. 2675–2692.
- [3] Baur W.H. 1980. Straight Si -O- Si bridging bonds do exist in silicates and silicon dioxide polymorphs. *Acta Crystallogr. Sect. B*. Vol. 36, pp. 2198–2202.
- [4] Bubnov M.M., Semjonov S.L., Likhachev M.E., Dianov E.M., Khopin V.F., Salganskii M.Y., Guryanov A.N., Fajardo J.C., Kuksenkov D.V., Koh J., Mazumder P. 2004. On the Origin of Excess Loss in Highly GeO Doped Single-Mode MCVD Fibers. *IEEE Photonics Technol. Lett.* Vol. 16, pp. 1870–1872.
- [5] Chmel A. and Sochivkin G.M. 1986. On formation of structural defects responsible for the 606 cm<sup>-1</sup> line in Raman spectrum of vitrum of vitreous SiO<sub>2</sub>. *Solid State Commun.* Vol. 58, pp. 363–365.
- [6] Friebele E., Griscom D., Stapelbroek M. and Weeks R. 1979. Fundamental Defect Centers in Glass: The Peroxy Radical in Irradiated, High-Purity, Fused Silica. *Phys. Rev. Lett.* Vol. 42, pp. 1346–1349.
- [7] Galeener F. 1979. Band limits and the vibrational spectra of tetrahedral glasses. *Phys. Rev. B*. Vol. 19, pp. 4292–4297.
- [8] Galeener F.L. 1982. Planar rings in vitreous silica. *J. Non. Cryst. Solids*, Vol. 49, pp. 53–62.
- [9] Gillet P., Le Cléac'h A. and Madon M. 1990. High-temperature raman spectroscopy of SiO<sub>2</sub> and GeO<sub>2</sub> Polymorphs: Anharmonicity and thermodynamic properties at high-temperatures. *J. Geophys. Res.* Vol. 95, p.21635.
- [10] Jr. J.C.M. and Galeener F.L. 1980. Thermal equilibration of raman active defects in vitreous silica. *J. Non. Cryst. Solids*, Vol. 37, pp. 71–84.
- [11] Lü H.-B., Xu S.-Z., Wang H.-J., Yuan X.-D., Zhao C. and Fu Y.Q. 2014. Evolution of Oxygen Deficiency Center on Fused Silica Surface Irradiated by Ultraviolet Laser and Posttreatment. *Adv. Condens. Matter Phys.* Pp. 1–4.
- [12] MacChesney J. 2000. MCVD: Its origin and subsequent development. *IEEE J. Sel. Top. Quantum Electron.* Vol. 6, pp. 1305–1306.
- [13] Martinez V., Parc R. Le, Martinet C., Champagnon B. 2003. Structural studies of germanium doped silica glasses: the role of the fictive temperature. *Opt. Mater. (Amst)*. Vol. 24, pp. 59–62.
- [14] McMillan P.F. 1980. Structural studies of silicate glasses and melts-applications and limitations of Raman spectroscopy Vol. 69.
- [15] McMillan P.F., Poe B.T., Gillet P.H. and Reynard B. 1994. A study of SiO<sub>2</sub> glass and supercooled liquid to 1950 K via high-temperature Raman spectroscopy. *Geochim. Cosmochim. Acta*, Vol. 58, pp. 3653–3664.





- [16] Nagel S.R., MacChesney J.B., Walker K.L. 1982. An Overview of the Modified Chemical Vapor Deposition (MCVD) Process and Performance. *IEEE Trans. Microw. Theory Tech.* Vol. 30, pp. 305–322.
- [17] Pasquarello A., Car R. 1998. Identification of Raman Defect Lines as Signatures of Ring Structures in Vitreous Silica. *Phys. Rev. Lett.* Vol. 80, pp. 5145–5147.
- [18] Revesz A.G. and Walrafen G.E. 1983. Structural interpretations for some Raman lines from vitreous silica. *J. Non. Cryst. Solids*, Vol. 54, pp. 323–333.
- [19] Salh R. 2011. *Crystalline Silicon - Properties and Uses*, InTech.
- [20] Sato T. and Suda J. 1998. Lattice Dynamics and Temperature Dependence of the Linewidth of the First-Order Raman Spectra for Sintered Hexagonal GeO<sub>2</sub> Crystalline. *J. Phys. Soc. Japan*, Vol. 67, pp. 3809–3815.
- [21] Shafiqah A.S.S., Amin Y.M., Nor R.M., Tamchek N. and Bradley D.A. 2015. Enhanced {TL} response due to radiation induced defects in Ge-doped silica preforms. *Radiat. Phys. Chem.* Vol. 111, pp. 87–90.
- [22] Shen N., Matthews M.J., Elhadj S., Miller P.E., Nelson A.J. and Hamilton J. 2013. Correlating optical damage threshold with intrinsic defect populations in fused silica as a function of heat treatment temperature. *J. Phys. D. Appl. Phys.* Vol. 46, p. 165305.
- [23] Simpkins P.G., Greenberg-Kosinski S. and MacChesney J.B. 1979. Thermophoresis: The mass transfer mechanism in modified chemical vapor deposition. *J. Appl. Phys.* Vol. 50, p. 5676.
- [24] Skuja L. 1998. Optically active oxygen-deficiency-related centers in amorphous silicon dioxide. *J. Non. Cryst. Solids*, Vol. 239, pp. 16–48.
- [25] Vaccaro G., Buscarino G., Agnello S., Messina G., Carpanese M. and Gelardi F.M. 2010. Structural properties of the range-II- and range-III order in amorphous-SiO<sub>2</sub> probed by electron paramagnetic resonance and Raman spectroscopy. *Eur. Phys. J. B.* Vol. 76, pp. 197–201.
- [26] Wood D., Walker K., MacChesney J., Simpson J. and Csencsits R. 1987. Germanium chemistry in the MCVD process for optical fiber fabrication. *J. Light. Technol.* Vol. 5, pp. 277–285.